

# Raman Scattering Study of Sodium Di-*n*-pentyl Phosphate Aggregates and Water Content Dependence of Conformation about P-O Bonds in Coagel Phases

Hirofumi Okabayashi,\*† Keijiro Taga,† Kiyotaka Miyagai,† Toshiyuki Uehara,† Tadayoshi Yoshida,† and Etsuo Nishio†

Department of Applied Chemistry, Nagoya Institute of Technology, Gokiso-cho, Showa-ku, Nagoya 466, Japan, and Osaka Branch, Perkin-Elmer Japan Company Ltd., Toyotsu, Suita, Osaka 564, Japan  
(Received: August 10, 1990; In Final Form: May 22, 1991)

For anhydrous sodium di-*n*-pentyl phosphate (DPP) in the solid state and the DPP-H<sub>2</sub>O system, the Raman scattering spectra due to the accordion vibration mode were investigated in the temperature range -80-100 °C. For anhydrous DPP, the GG form about the P-O bonds was stabilized at lower temperatures. In the coagel phases of DPP-H<sub>2</sub>O, preferential stabilization of a specific rotational isomer about the P-O bonds occurred and the species of stabilized conformer was dependent on the water content; for the 7:3 DPP-H<sub>2</sub>O coagel the TT form was stabilized, while for the 8:2 DPP-H<sub>2</sub>O coagel the GT form was preferentially stabilized. The stabilization of such a specific conformer was also reflected in some conformationally sensitive Raman bands in the higher frequency region.

## Introduction

Considerable attention has been given to structural studies of dialkyl phosphates.<sup>1-11</sup> These studies have served as a pathway toward the understanding of the physical properties of phospholipid aggregates when they are used as a membrane model. The conformation of simple dialkyl phosphate anions has been investigated by infrared absorption and Raman scattering<sup>12,13</sup> and nuclear magnetic resonance<sup>14,15</sup> spectroscopic methods. X-ray crystallographic analysis<sup>16</sup> of a single crystal of barium diethyl phosphate (BaDEP) has been made and has provided the detailed geometrical parameters of this molecule in the crystalline state.

Brown et al.<sup>17</sup> have reported the Raman spectra and normal coordinate analysis of the rotational isomers for the diethyl phosphate anion. Their results have indicated that the calculated frequencies of the symmetric and antisymmetric O-P-O stretching, the symmetric and antisymmetric PO<sub>2</sub><sup>-</sup> stretching, and the C-C stretching modes are sensitive to the P-O and C-O dihedral angles.

The vibrational bands due to the skeletal deformation modes appearing in the low-frequency region provide direct information on the molecular conformation.<sup>18-25</sup> The accordion-like vibrational mode arising from the all-trans hydrocarbon chain is a powerful indicator of conformational change upon alteration of the aggregate structures.<sup>21,23</sup>

In this study, we report the Raman spectra of the binary sodium di-*n*-pentyl phosphate-water system and discuss the sensitivity of the accordion-like vibrational frequency in relation to the conformational change about the P-O bonds for the polar head in the solid and coagel states.

## Experimental Section

**Materials.** The sample of sodium di-*n*-pentyl phosphate (DPP) was prepared as follows. Di-*n*-pentyl phosphorochloridate, (C<sub>5</sub>H<sub>11</sub>(CH<sub>2</sub>)<sub>4</sub>O)<sub>2</sub>P(O)Cl, was synthesized by using phosphoryl chloride and 1-pentanol according to a method similar to that of Saunders et al.<sup>26</sup> The fraction of bp 120 °C/4 mmHg was collected. Di-*n*-pentyl phosphorochloridate was treated with water, and the resulting HCl was pumped off to yield phosphoric acid di-*n*-pentyl ester, (CH<sub>3</sub>(CH<sub>2</sub>)<sub>4</sub>O)<sub>2</sub>P(O)OH. The ester was neutralized with aqueous sodium hydroxide, and the sodium salt was recrystallized in aqueous acetone. The identification of DPP was made by <sup>13</sup>C NMR spectral and elemental analysis. Since the sodium salt was hygroscopic, the barium salt was used for the elemental analysis. Anal. Calcd C<sub>20</sub>H<sub>44</sub>O<sub>8</sub>P<sub>2</sub>Ba: C, 39.26; H, 7.25. Found: C, 39.06; H, 7.47. The liquid crystalline samples of DPP were prepared by heating of the 7:3 and 8:2 DPP-H<sub>2</sub>O

TABLE I: Force Constants for DPP<sup>a</sup>

force constant	value	force constant	value
K(C-H), CH <sub>3</sub>	4.250	H(O=P=O)	0.349
K(C-H), CH <sub>2</sub>	4.000	H(O=P=O)	0.210
K(C-C)	2.500	F(H-C-H)	0.200
K(C-O)	3.500	F(C-C-H)	0.540
K(P-O)	2.560	F(C-C-O)	0.650
K(P=O)	7.500	F(O-C-H)	0.756
H(H-C-H), CH <sub>3</sub>	0.372	F(C-O-P)	0.300
H(H-C-H), CH <sub>2</sub>	0.338	F(C-C-C)	0.500 <sup>b</sup>
H(C-C-H), CH <sub>3</sub>	0.210	F(O-P-O)	0.558
H(C-C-H), CCH <sub>2</sub>	0.140	Y(C-C)	0.096
H(C-C-O)	0.500 <sup>b</sup>	Y(C-O)	0.038
H(O-C-H)	0.253	Y(P-O)	0.080
H(C-O-P)	0.207	κ(PO <sub>4</sub> )	0.374
H(C-C-C)	0.500 <sup>b</sup>	p(C-H)	-0.090
H(O-P-O)	0.375	p(P=O)	-0.350

<sup>a</sup> The units of the Urey-Bradley force constants are mdyne Å<sup>-1</sup> for stretching, K; bending, H; repulsion, F; and bond interaction, p; and mdyne Å for torsion, Y; and intramolecular tension, κ. <sup>b</sup> The values are assumed to be the same values of H(C-O-C) and F(C-O-C), respectively.<sup>44</sup>

(wt %) mixtures, which are termed S I and S II, respectively. DPP was dehydrated by vacuum drying in an oil bath at 150 °C. In

- (1) Nakagaki, M.; Handa, T. *Bull. Chem. Soc. Jpn.* **1975**, *48*, 630.
- (2) Kunitake, T.; Okahata, Y. *J. Am. Chem. Soc.* **1977**, *99*, 3860.
- (3) Kunitake, T.; Okahata, Y. *Bull. Chem. Soc. Jpn.* **1978**, *51*, 1877.
- (4) Kano, K.; Romero, A.; Djermouni, B.; Ache, H. J.; Fendler, J. H. *J. Am. Chem. Soc.* **1979**, *101*, 4030.
- (5) Shimomura, M.; Kunitake, T. *J. Am. Chem. Soc.* **1982**, *104*, 1757.
- (6) Wagenaar, A.; Rupert, L. A. M.; Engberts, J. B. F. N.; Hoekstra, D. *J. Org. Chem.* **1989**, *54*, 2638.
- (7) Sudhölter, E. J. R.; Engberts, J. B. F. N.; Hoekstra, D. *J. Am. Chem. Soc.* **1980**, *102*, 2467.
- (8) Sudhölter, E. J. R.; de Grip, W. J.; Engberts, J. B. F. N. *J. Am. Chem. Soc.* **1982**, *104*, 1069.
- (9) Rupert, L. A. M.; Hoekstra, D.; Engberts, J. B. F. N. *J. Am. Chem. Soc.* **1985**, *107*, 2628.
- (10) Rupert, L. A. M.; Van Breemen, J. F. C.; Van Bruggen, E. F. J.; Engberts, J. B. F. N.; Hoekstra, D. *J. Membr. Biol.* **1987**, *95*, 255.
- (11) Rupert, L. A. M.; Hoekstra, D.; Engberts, J. B. F. N. *J. Colloid Interface Sci.* **1987**, *120*, 125.
- (12) Shimanouchi, T.; Tsuboi, M.; Kyogoku, Y. *Adv. Chem. Phys.* **1964**, *7*, 435.
- (13) Okabayashi, H.; Yoshida, T.; Ikeda, T.; Matsuura, H.; Kitagawa, T. *J. Am. Chem. Soc.* **1982**, *104*, 5399.
- (14) Tsuboi, M.; Kuriyagawa, F.; Matsuo, K.; Kyogoku, Y. *Bull. Chem. Soc. Jpn.* **1967**, *40*, 1813.
- (15) Kamo, O.; Matsushita, K.; Terada, Y.; Yoshida, T.; Okabayashi, H. *Chem. Scr.* **1984**, *23*, 189.
- (16) Kyogoku, Y.; Iitaka, Y. *Acta Crystallogr.* **1966**, *21*, 49.
- (17) Brown, E. B.; Brown, K. G.; Person, W. B. *J. Raman Spectrosc.* **1981**, *11*, 356.

\* Nagoya Institute of Technology.

† Perkin-Elmer Japan Co. Ltd.

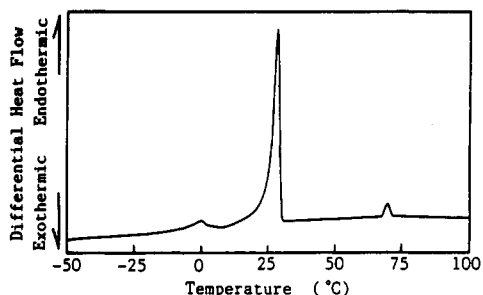


Figure 1. Differential scanning calorimetry of S II in the liquid crystalline state.

TABLE II: Phase Transition Temperature ( $T_i$ ) and  $\Delta H$  of DPP in the Liquid Crystal

	$T_i$ , °C	$\Delta H$ , J/g
SI	7.6	52.32
	84.2	9.95
SII	0.0	8.59
	28.6	60.20
	69.9	2.12

the dehydrated DPP, S III, water was undetectable by infrared spectroscopy.

**Calorimetry.** The thermotropic transition temperature of the lyotropic DPP liquid crystal was determined with a differential scanning calorimeter (Perkin-Elmer DSC-7 series) which was scanned at a rate of 5 °C/min by using a volatile pan.

**Raman Scattering Measurements.** The Raman scattering spectra were measured by the 514.5-nm line of an Ar ion laser (NEC GLG-3200) and were recorded on a JEOL JRS-400D Raman spectrometer. For measurements in the temperature range -80 to 100 °C, DPP in a capillary was placed in a variable-temperature capillary cell system (JEOL RS-VTC41).

**Normal Coordinate Calculations.** The normal vibrations of DPP were calculated by the use of the modified Urey-Bradley force field. A HITAC M-260K system in the Center of Information Processing Education of the Nagoya Institute of Technology was used for the calculations, using the program NCTB prepared by Shimanouchi et al.<sup>27</sup> Structural parameters of BaDEP determined by X-ray analysis<sup>16</sup> were used for DPP;  $r(\text{P}=\text{O}) = 1.51 \text{ \AA}$ ,  $r(\text{P}-\text{O}) = 1.605 \text{ \AA}$ ,  $r(\text{C}-\text{O}) = 1.455 \text{ \AA}$ ,  $r(\text{C}-\text{C}) = 1.51 \text{ \AA}$ ,  $r(\text{C}-\text{H}) = 1.09 \text{ \AA}$ , and  $\angle\text{COP} = 120^\circ$ . It was assumed that the other valence angles were tetrahedral and that the internal rotation angles were 60° for the gauche (G) form and 180° for the trans (T) form.

Force constants were taken from those of BaDEP.<sup>28</sup> The force constants were modified by the least-squares method to obtain the best fit between the calculated and the observed frequencies of the solid state (S III at -80 °C). These corrected force constants were then used for normal coordinate calculations of the other possible rotational isomers. The force constants used are listed in Table I. Assignments were based on the potential energy distributions.

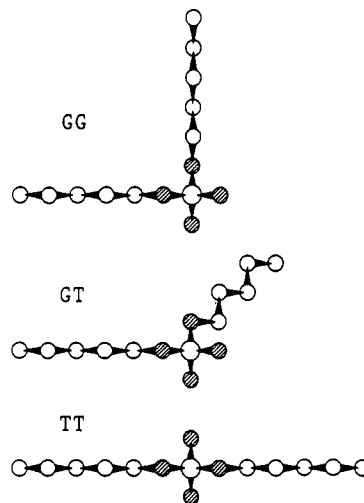


Figure 2. Schematic representation of three rotational isomers (GG, GT, and TT) about the P-O bonds. The conformations about every  $\text{CH}_2-\text{CH}_2$  bond and two  $\text{CH}_2-\text{O}$  bonds were assumed to be in the trans conformation.

## Results and Discussion

**Thermotropic Properties of DPP-H<sub>2</sub>O.** Differential scanning calorimetric measurements were made of the DPP-H<sub>2</sub>O system (Figure 1). The temperatures of the thermotropic phase transition are listed in Table II with the  $\Delta H$  values being calculated from the peak area. A polarized microscope with a temperature-variable stage was used to investigate the phase feature.

Above the phase transition point at 84.2 °C for S I (7:3 DPP-H<sub>2</sub>O mixture), the phase is in the isotropic state, while in the range 7.6–84.2 °C it is in the lyotropic liquid crystalline state and below 7.6 °C it is in the coagel state. For S II (8:2 DPP-H<sub>2</sub>O mixture), the phases are in the isotropic state above 69.9 °C, in the lyotropic state in the temperature range 28.6–69.9 °C, and in the coagel state below 28.6 °C.

For the sodium di-*n*-butyl phosphate (DBP)-water system in the lyotropic state, the existence of a lamellar structure was suggested by the observation that the <sup>31</sup>P NMR line shape had a low-field shoulder.<sup>29</sup> For the DPP used in this study, a lamellar structure was also confirmed by X-ray diffraction.<sup>30</sup>

**Raman Spectra of DPP-H<sub>2</sub>O and Conformational Preferences in the Coagels.** For S I, S II, and S III, the temperature dependence of the Raman spectra was investigated in the region 100–3000  $\text{cm}^{-1}$ . It was found that the lyotropic to coagel transition brings about a marked change in the Raman spectra with the spectral features being strongly dependent upon the water content. For the binary system of surfactant-water, it has been considered that crystals of hydrated surfactant molecules are formed in the coagel phases.<sup>31</sup> Hydrocarbon chains take up the all-trans conformation in the solid state.<sup>21,23</sup> Therefore, we may assume that the *n*-pentyl chains of a DPP molecule take up the all-trans conformation in the dehydrated solid state.

Normal coordinate analysis was made to explain the Raman spectra of the coagels and dehydrated samples. In the present calculations, it was assumed that conformers about every C-H<sub>2</sub>-CH<sub>2</sub> bond and about the two CH<sub>2</sub>-O bonds are in the trans conformation. Although three conformers of trans (T), gauche (G), and gauche' (G') about the phosphodiester P-O bonds were considered, only three molecular forms (GG, GT, and TT) were used for the calculations (Figure 2). The four mirror images (G'G', G'T, TG, and TG') were omitted, and the GG' and G'G forms were also omitted because of their instability due to the steric hindrance.

(18) Mizushima, S.; Shimanouchi, T. *J. Am. Chem. Soc.* **1949**, *71*, 1320.

(19) Schaufele, R. F.; Shimanouchi, T. *J. Chem. Phys.* **1967**, *47*, 3605.

(20) Schaufele, R. F. *J. Chem. Phys.* **1968**, *49*, 4168.

(21) Okabayashi, H.; Okuyama, M.; Kitagawa, T. *Bull. Chem. Soc. Jpn.* **1975**, *48*, 2264.

(22) Okabayashi, H.; Abe, M. *J. Phys. Chem.* **1980**, *84*, 999.

(23) Okabayashi, H.; Taga, K.; Tsukamoto, K.; Tamaoki, H.; Yoshida, T.; Matsuura, H. *Chem. Scr.* **1985**, *25*, 153.

(24) Tsukamoto, K.; Ohshima, K.; Taga, K.; Okabayashi, H.; Matsuura, H. *J. Chem. Soc., Faraday Trans. 1* **1987**, *83*, 786.

(25) Okabayashi, H.; Tsukamoto, K.; Ohshima, K.; Taga, K.; Nishio, E. *J. Chem. Soc., Faraday Trans. 1* **1988**, *84*, 1639.

(26) Saunders, B. C.; Stacey, G. J.; Wild, F.; Wilding, I. G. E. *J. Chem. Soc.* **1948**, 699.

(27) Shimanouchi, T. *Computer program for normal coordinate treatment of polyatomic molecules*; University of Tokyo: Tokyo, 1968.

(28) Taga, K.; Miyagai, K.; Hirabayashi, N.; Yoshida, T.; Okabayashi, H. *J. Mol. Struct.* **1991**, *245*, 1.

(29) Chachaty, C.; Quaegebeur, J. P. *J. Phys. Chem.* **1983**, *87*, 4341.

(30) Okabayashi, H.; Taga, K. Unpublished data.

(31) Kodama, M.; Seki, S. *Netsu Sokutei* **1984**, *11*, 104.

(32) Garrigou-Lagrange, C.; Bouloussam, O.; Clement, S. *Can. J. Spectrosc.* **1976**, *21*, 75.

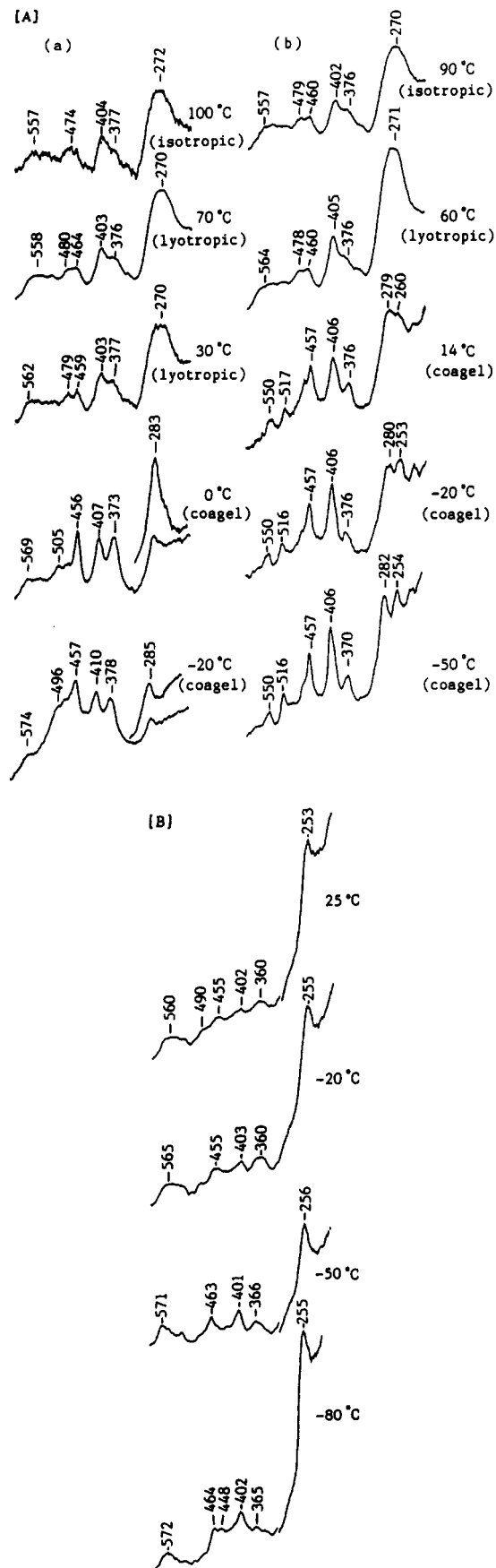


**Figure 3.** Raman spectra: [A] S I (a) and S II (b) in the low-frequency region for the isotropic, lyotropic, and coagel phases; [B] S III at low temperatures.

**A. The 200–600-cm<sup>-1</sup> Region.** Figure 3A shows the Raman spectra of S I and S II in the 200–600-cm<sup>-1</sup> region at different temperatures. In the isotropic and liquid crystalline states, the

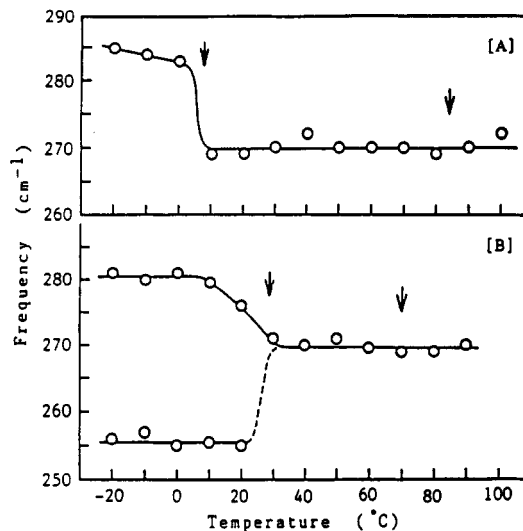


**Figure 4.** Temperature dependence of the Raman band frequency in the accordion vibrational region for [A] S I and [B] S II. The arrows designate the phase transition temperatures.

Raman band at 270–272 cm<sup>-1</sup> is assigned to the accordion vibrational modes arising from the all-trans *n*-pentyl chains.<sup>13</sup> The bands at 376–377, 402–405, 459–464, and 557–564 cm<sup>-1</sup> are also observed in common and arise from the deformational vibrations of a phosphate group coupled with the CCC deformational modes of the hydrocarbon chains.

Figure 4 shows the temperature dependence of the Raman band in the accordion-like vibrational region. In the isotropic and lyotropic states, the accordion-like vibrational bands for S I and S II have almost the same frequencies at different temperatures, although the bands are very broad. For S I and S II, the phase transition from the lyotropic to the coagel phase brings about a marked difference in their spectral features. It should be noted that the accordion-like vibrational bands appear at 283–285 cm<sup>-1</sup> for the coagel S I and at 253–260 and 279–282 cm<sup>-1</sup> for the coagel S II, while the accordion-like vibrational band for S III is observed at 253–256 cm<sup>-1</sup> (Figure 3B). Therefore, the behavior of the accordion-like vibrational mode is found to depend strongly upon the water content of the samples.

Table III lists the calculated skeletal deformational frequencies of DPP in the 200–600-cm<sup>-1</sup> region, together with the assignments and the observed frequencies. Results indicate reasonable agreement between the calculated values of the three conformers and the observed frequencies for the three samples. The Raman band at 253–256 cm<sup>-1</sup> for S III in the dehydrated solid state is assigned to the GG form. Since the gauche configuration with regard to the P–O bonds has been confirmed by X-ray crystallographic analysis of BaDEP,<sup>16</sup> this assignment seems to be reasonable. The accordion-like vibrational band at 283–285 cm<sup>-1</sup> observed for the coagel S I can be assigned to the TT form. For the coagel S II, the Raman bands at 253–260 and 279–282 cm<sup>-1</sup> are assigned to the accordion-like vibrations arising from the GT form. The former band arises from the accordion-like vibrational mode of one of the two all-trans-*n*-pentyl chains, which is in the gauche configuration with respect to the P–O bond; the latter band arises from the accordion-like vibrational mode of another extended chain in the trans configuration to the P–O bond. This result indicates that the conformation about the P–O bonds strongly depends upon the water content in the two coagel states. Thus, for S I the lyotropic to coagel phase transition brings about the preferential stabilization of the TT form, while for S II the GT form is stabilized by the phase transition.

As expected from the calculated vibrational frequencies of dimethyl phosphate (DMP) and DEP,<sup>12,17,33</sup> the deformational vibrations of the phosphate group depend upon the phosphodiester

TABLE III: Observed and Calculated Frequencies (cm<sup>-1</sup>) of DPP in the 200–600-cm<sup>-1</sup> Region

obsd <sup>a</sup>			calcd			assignment <sup>b</sup>
S I <sub>coagel</sub> (-20 °C)	S II <sub>coagel</sub> (-20 °C)	S III <sub>dehyd</sub> (-80 °C)	TT	GT	GG	
574vw	575vw,b	572w	578	572	559	δOPO + δ <sub>s</sub> skel (TT, GT), δOPO (GG)
	550w	560vw,b		548	558	rPO <sub>2</sub> <sup>-</sup> (GT, GG)
530sh		540vw	524		530	rPO <sub>2</sub> <sup>-</sup> (TT), δ <sub>s</sub> skel (GG)
			522			δ <sub>s</sub> skel (TT)
	516w			502		δ <sub>s</sub> skel (GT)
496vw	490vw,b	480vw,b	481	487	476	δ <sub>s</sub> skel (TT), rPO <sub>2</sub> <sup>-</sup> + δ <sub>s</sub> skel (GT), wPO <sub>2</sub> <sup>-</sup> (GG)
470vw	470sh	464w	454	461	460	sPO <sub>2</sub> <sup>-</sup> (TT), δ <sub>s</sub> skel (GT, GG)
457m	457m		445	447		δ <sub>s</sub> skel (TT), δ <sub>s</sub> skel + sPO <sub>2</sub> <sup>-</sup> (GT)
		448w			439	δ <sub>s</sub> skel (GG)
		402w	411	395	396	tPO <sub>2</sub> <sup>-</sup> (TT, GT), sPO <sub>2</sub> <sup>-</sup> + tPO <sub>2</sub> <sup>-</sup> (GG)
378m	370w	365vw,b	369	373	373	sPO <sub>2</sub> <sup>-</sup> + δOPO (TT, GT), tPO <sub>2</sub> <sup>-</sup> + sPO <sub>2</sub> <sup>-</sup> (GG)
285m	282m		298	265		
	254m	255s		250	251	δ <sub>s</sub> skel (accordion modes)
				249		
			242	243		τCC (TT, GT, GG)
220vw,b	220vw,b		215	200	211	δPOC (TT), δ <sub>s</sub> skel + δPOC (GT), δ <sub>s</sub> skel (GG)

<sup>a</sup>s, strong; m, medium; w, weak, v, very; sh, shoulder; b, broad. <sup>b</sup>δ, deformation; a, antisymmetric; s, symmetric; r, rocking; w, wagging; s, scissoring; t, twisting; τ, torsion.

TABLE IV: Observed Raman and Calculated Frequencies (cm<sup>-1</sup>) for DPP in the Lyotropic, Coagel, and Dehydrated States in the 700–1250-cm<sup>-1</sup> Region

obsd <sup>a</sup>				calcd			assignment <sup>b</sup>
S I <sub>lyotr</sub> (30 °C)	S I <sub>coagel</sub> (-20 °C)	S II <sub>coagel</sub> (-20 °C)	S III <sub>dehyd</sub> (-80 °C)	TT	GT	GG	
1250w	1247w	1246w	1248w	{ 1232 1234	{ 1239 1234 1231	{ 1242 1234 1231	{ ν <sub>s</sub> PO <sub>2</sub> <sup>-</sup> wCH <sub>2</sub> ν <sub>s</sub> PO <sub>2</sub> <sup>-</sup> + wCH <sub>2</sub>
1220vw	1219w	1218w	1220vw	{ 1225 1213 1204	{ 1224 1213 1204	{ 1224 1213 1204	{ wCH <sub>2</sub>
1151vw	1152vw	1153m	1153w	{ 1156 1153	{ 1156 1153	{ 1156 1153	{ tCH <sub>2</sub>
1118s	1122m	1123m	1118s	{ 1121 1126	{ 1121 1116	{ 1121 1114	{ νCO
1111vs	1101s	1098s		{ 1100 1099 1095 1091	{ 1109 1097 1096 1092	{ 1109 1098 1095 1093	{ ν <sub>s</sub> PO <sub>2</sub> <sup>-</sup> + νCC νCC ν <sub>s</sub> PO <sub>2</sub> <sup>-</sup> + νCC
1076m	1070m	1075m		{ 1067 1058	{ 1067 1057	{ 1067 1057	{ νCC
1062m			1061m	{ 1057	{ 1057	{ 1057	{ rCH <sub>3</sub>
1030vw	1032m	1034vw	1030w				
992vw			996vw				
975vw	985w	977w		959	959	959	
930vw	928vw	930vw	930vw	948	948	948	
898m			899m				
880m		876s					rCH <sub>2</sub>
865m	868s		865m				
842m		848m		834	834	834	
814s	822s	821s	814m	818	808	802	ν <sub>s</sub> OPO
				810	820	825	ν <sub>s</sub> OPO + wPO <sub>2</sub> <sup>-</sup>
	770vvw	773vvw					
759m	757w	758w	759w	751	751	751	
726w	728vw	726vw	726w	723	723	723	rCH <sub>2</sub>

<sup>a,b</sup>See footnotes to Table III.

torsional angles. Table III also lists the calculated deformational frequencies of the DPP phosphate group and their assignments. The calculated results indicate the frequency differences due to the different configurations about the P-O bonds. For S I, S II, and S III, the Raman bands at 365–378 and 402–410 cm<sup>-1</sup> mainly come from the PO<sub>2</sub><sup>-</sup> twisting and the OPO deformation vibrational modes, respectively. The Raman band at 456–457 cm<sup>-1</sup> for the coagel S I is assigned to the PO<sub>2</sub><sup>-</sup> wagging mode coupled with the CCC skeletal deformation and the 457-cm<sup>-1</sup> band of the coagel S II to the PO<sub>2</sub><sup>-</sup> scissoring vibration. The Raman band at 448 cm<sup>-1</sup> observed for S III at -80 °C is due to the CCC skeletal deformation coupled with the PO<sub>2</sub><sup>-</sup> rocking vibration and may be characteristic of the GG form. For the coagel S II, the Raman band at 516–517 cm<sup>-1</sup> arising from the CCC skeletal deformation increases in intensity at lower temperatures and may be characteristic of the GT form.

These observations in the low-frequency region directly reveal that the extent of hydration of the phosphate group affects the conformational preferences of phosphodiester torsional angles of DPP.

**B. The 700–1250-cm<sup>-1</sup> Region.** Table IV lists the calculated frequencies of symmetric and antisymmetric O-P-O stretching (ν<sub>s</sub>OPO and ν<sub>a</sub>OPO), symmetric and antisymmetric PO<sub>2</sub><sup>-</sup> (ν<sub>s</sub>PO<sub>2</sub><sup>-</sup> and ν<sub>a</sub>PO<sub>2</sub><sup>-</sup>), C-C stretching (νCC), and the characteristic vibrational modes of the CH<sub>3</sub> and CH<sub>2</sub> groups for DPP in the 700–1250-cm<sup>-1</sup> region, together with the observed frequencies and assignments.

The present calculations for DPP predict that the GG form about the P-O bonds appears at higher frequency for the ν<sub>s</sub>OPO mode relative to the ν<sub>s</sub>OPO mode, while the reverse is true for the TT form, as is seen in Table IV. This result is consistent with that obtained from the vibrational studies for DMP and DEP.<sup>12,17</sup>

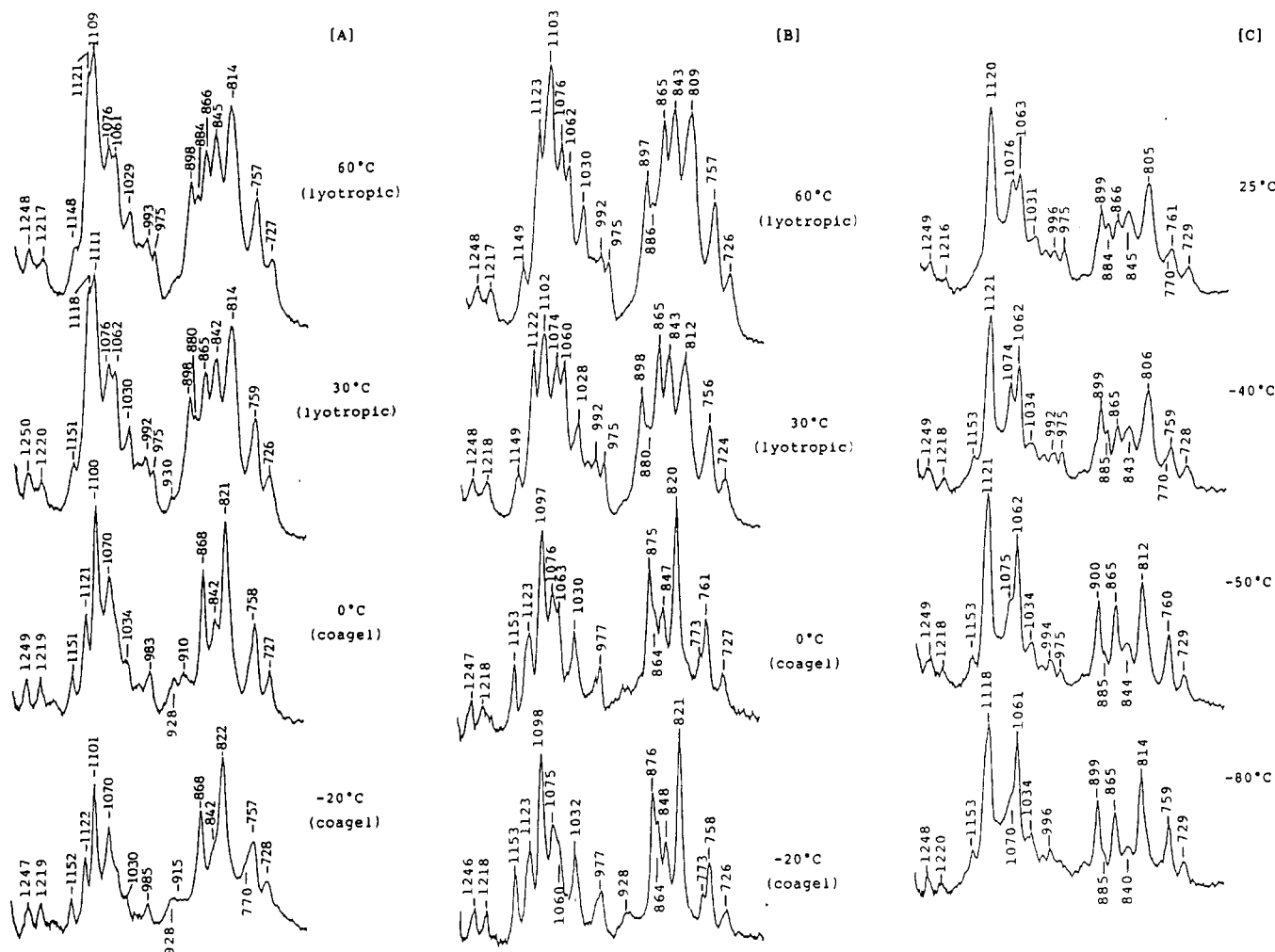


**Figure 5.** Raman spectra of [A] S I and [B] S II in the lyotropic and coagel phases and [C] S III at low temperature in the 700–1200-cm<sup>-1</sup> region.

The Raman spectra of S I and S II in the lyotropic and coagel phases and those of S III at low temperature in the 700–950-cm<sup>-1</sup> region are shown in Figure 5.

The Raman band at 809–814 cm<sup>-1</sup> is observed in common for S I and S II in the lyotropic state. This band is broad compared with the other bands. However, this band disappears upon the phase transition from the lyotropic to the coagel phase and a new band at 820–822 cm<sup>-1</sup> appears. For S III, the band at 805 cm<sup>-1</sup> that is observed at 25 °C is gradually shifted to a higher frequency at 814 cm<sup>-1</sup> when the sample is cooled at -80 °C. The band at 814 cm<sup>-1</sup> obviously arises from the GG form. Therefore, the bands at 820–822 cm<sup>-1</sup> in the coagels S I and S II can be ascribed to the TT and GT forms. The Raman band at 814 cm<sup>-1</sup> arising from the GG form is at a lower frequency than that at 822 cm<sup>-1</sup> for the TT form. On the basis of normal coordinate analysis and consistency with the experimental results, the strong Raman bands at 809–822 cm<sup>-1</sup> for S I and S II and at 805–814 cm<sup>-1</sup> for S III may be assigned to  $\nu_5$ OPO.

The present normal coordinate analysis also shows that the CH<sub>2</sub> rocking (rCH<sub>2</sub>) modes appear in common for the three conformers at 723, 751, 834, and 948 cm<sup>-1</sup> (Table IV). Therefore, the Raman bands of S I, S II, and S III appearing in the regions 720–780 and 840–950 cm<sup>-1</sup> may be assigned to the rCH<sub>2</sub> modes of the *n*-pentyl chains. These assignments are consistent with those of *n*-paraffins.<sup>34</sup>

For the Raman bands in the 720–780-cm<sup>-1</sup> region, there is no marked difference in the vibrational frequency among S I, S II, and S III. However, it should be noted that a splitting of the rCH<sub>2</sub> modes occurs for the coagels S I and S II. Obviously, upon the lyotropic to coagel transition, the Raman band at 770–773 cm<sup>-1</sup>

newly appears for S I and S II. For S III, such splitting occurs at higher temperatures and the band at 770 cm<sup>-1</sup> disappears when the temperature is lowered. Thus, the 770–773-cm<sup>-1</sup> band should be due to the GT and TT forms.

The Raman band at 897–898 cm<sup>-1</sup>, which corresponds to the prominent band at 899–900 cm<sup>-1</sup> for S III due to the GG form, disappears in the coagels S I and S II. For S III, the Raman band at 884–885 cm<sup>-1</sup> decreases in intensity as the sample is cooled below 25 °C. The corresponding Raman band is not observed in the coagel S I in which the TT form is predominantly stabilized. On the other hand, in the coagel S II the Raman band at 875–876 cm<sup>-1</sup> is intensified, reflecting the stabilization of the GT form at low temperatures. This band may correspond to the 884–885-cm<sup>-1</sup> band for S III above 25 °C.

The Raman band at 840–845 cm<sup>-1</sup> decreases in intensity with a decrease in temperature for both S III and coagel S I, while for coagel S II the corresponding band at 843–848 cm<sup>-1</sup> has medium intensity in the temperature range -50 to -20 °C. Therefore, this band may be assigned the characteristics of the GT form. Thus, the conformational preferences about the P-O bonds, depending upon the water content, are reflected markedly in the rCH<sub>2</sub> regions. For S I and S II in the lyotropic state, the Raman bands at 842–845 and 897–898 cm<sup>-1</sup> are intensified, indicating that the GT and GG forms are stabilized.

As expected from the calculated results (Table IV), there exists a possibility for overlapping of the  $\nu$ CO,  $\nu$ CC, twisting CH<sub>2</sub> (tCH<sub>2</sub>), and  $\nu_5$ PO<sub>2</sub><sup>-</sup> modes because of a splitting of the  $\nu_5$ PO<sub>2</sub><sup>-</sup> mode due to the coupling with the  $\nu$ CC modes. For S III, the Raman bands at 1063, 1076, and 1120 cm<sup>-1</sup> are prominent at 25 °C (Figure 5C). The strong bands at 1063 and 1076 cm<sup>-1</sup> arise from the  $\nu$ CC modes of the extended *n*-pentyl chains. The very strong and broad band at 1120 cm<sup>-1</sup> comes from  $\nu_5$ PO<sub>2</sub><sup>-</sup> overlapped with the  $\nu$ CO, tCH<sub>2</sub>, and  $\nu$ CC modes. The Raman spectral

(34) Snyder, R. G.; Schachtshneider, J. H. *Spectrochim. Acta* 1963, 19, 85.

features are also sensitive to the temperature. The Raman band at  $1076\text{ cm}^{-1}$  rapidly decreases in intensity as the temperature is lowered until it is observed as a shoulder at  $-80\text{ }^\circ\text{C}$ . This trend indicates that the TT or the GT form coexists for S III at  $25\text{ }^\circ\text{C}$ . Moreover, a decrease in temperature brings about an increase in intensity of the band at  $1061\text{--}1063\text{ cm}^{-1}$ . Therefore, stabilization of the GG form is also reflected in the spectral features in this region. The Raman band at  $1061\text{--}1063\text{ cm}^{-1}$  should be regarded as a characteristic of the GG form.

For the coagels S I and S II, prominent Raman bands at  $1028\text{--}1034$ ,  $1070\text{--}1076$ ,  $1097\text{--}1111$ ,  $1118\text{--}1123$ , and  $1148\text{--}1153\text{ cm}^{-1}$  are observed (Figure 5A,B) and assignments of these bands are summarized in Table IV. The band at  $1061\text{--}1063\text{ cm}^{-1}$  corresponding to S III disappears at lower temperatures. This behavior may indicate that the band at  $1070\text{--}1076\text{ cm}^{-1}$  is characteristic of the TT and GT forms. The strong Raman band at  $1097\text{--}1111\text{ cm}^{-1}$  for the coagels S I and S II, assigned to  $\nu_s\text{PO}_2^-$ , is lower in frequency compared with  $\nu_s\text{PO}_2^-$  at  $1118\text{ cm}^{-1}$  for S III. This lowering may be due to the difference in conformation about the P-O bonds.

Brown et al.<sup>17</sup> and Jayaram et al.<sup>33</sup> have already pointed out that the  $\nu_s\text{PO}_2^-$  band frequency depends upon the conformation about the P-O bonds. Conformation dependence of the  $\nu_s\text{PO}_2^-$  frequency is not so marked in the present calculation. The difference of the  $\nu_s\text{PO}_2^-$  frequency among three conformations may become smaller with an increased  $\text{CH}_2$  chain length owing to the coupling with the  $\nu\text{CC}$  modes.

The stabilization of a specific rotational isomer about the P-O bonds also reflects the Raman spectral feature in the region of  $\text{CH}_3$  rocking vibrations (Figure 5). For the lyotropic S I and S II, two Raman bands at  $975$  and  $992\text{--}993\text{ cm}^{-1}$  are observed in common. In the coagel S I, both bands disappear and the band at  $983\text{--}985\text{ cm}^{-1}$  appears, while in the coagel S II the band at  $977\text{ cm}^{-1}$  corresponding to the one at  $975\text{ cm}^{-1}$  increases in intensity. Therefore, the bands at  $983\text{--}985$  and  $977\text{ cm}^{-1}$  may be ascribed to the TT and GT forms, respectively. For the Raman bands at  $975$  and  $992\text{--}996\text{ cm}^{-1}$  observed for S III, temperature lowering results in an increase in intensity of the latter band. Thus, the band at  $992\text{--}996\text{ cm}^{-1}$  may arise from the GG form. Since it is predicted that the mode wagging  $\text{CH}_2$  ( $\omega\text{CH}_2$ ) should also appear at  $1200\text{--}1230\text{ cm}^{-1}$ , the  $\nu_a\text{PO}_2^-$  mode may be overlapped with this mode. This overlap makes it difficult to discuss the  $\nu_a\text{PO}_2^-$  modes in relation to the conformations about the P-O bonds.

Thus, the conformational preference about the phosphodiester torsional angle is reflected in the localized vibrational modes of the  $n$ -pentyl chains. This preference may come from the difference of the chain packing between the three samples, which provides the different environments of the  $\text{CH}_3$  and  $\text{CH}_2$  groups. In the present calculations, it is difficult to explain the Raman spectral features in the localized vibrational regions mentioned above.

**C. The  $1400\text{--}1500\text{-}$  and  $2800\text{--}3000\text{-cm}^{-1}$  Regions.** The  $\text{CH}_2$  scissoring ( $s\text{CH}_2$ ) band observed in the  $1400\text{--}1500\text{-cm}^{-1}$  region is sensitive to molecular interactions and is useful as a monitor of the packing state of the methylene chain in the gel or crystalline state.<sup>35,36</sup>

Figure 6A shows the temperature dependence of the Raman spectrum for S III in this region. Temperature lowering brings about a marked change in the spectral feature. The separations ( $\Delta\nu$ ) between the Raman bands at  $1443\text{--}1446$  and  $1453\text{--}1458\text{ cm}^{-1}$  gradually become larger with a decrease in temperature;  $\Delta\nu = 7\text{ cm}^{-1}$  at  $25\text{ }^\circ\text{C}$ ,  $10\text{ cm}^{-1}$  at  $-20\text{ }^\circ\text{C}$ ,  $12\text{ cm}^{-1}$  at  $-40\text{ }^\circ\text{C}$ , and  $15\text{ cm}^{-1}$  at  $-80\text{ }^\circ\text{C}$ . This behavior should be due to the change in the packing of the  $n$ -pentyl chains upon the preferential stabilization of the GG form. The spectral feature in this region also differs between the coagels S I and S II (Figure 6B). This difference may also reflect the difference in the chain packing between two coagel states, caused by stabilization of a specific isomer about the P-O bonds.

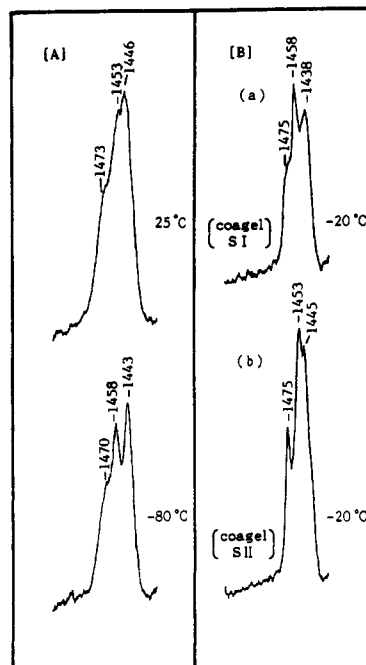


**Figure 6.** [A] Temperature dependence of the  $s\text{CH}_2$  Raman bands of S III ( $\Delta\nu$ :  $7\text{ cm}^{-1}$  at  $25\text{ }^\circ\text{C}$ ,  $10\text{ cm}^{-1}$  at  $-20\text{ }^\circ\text{C}$ ,  $12\text{ cm}^{-1}$  at  $-40\text{ }^\circ\text{C}$ , and  $15\text{ cm}^{-1}$  at  $-80\text{ }^\circ\text{C}$ ). [B] Raman spectra of coagels S I (a) and S II (b) at  $-20\text{ }^\circ\text{C}$  in the  $s\text{CH}_2$  region.

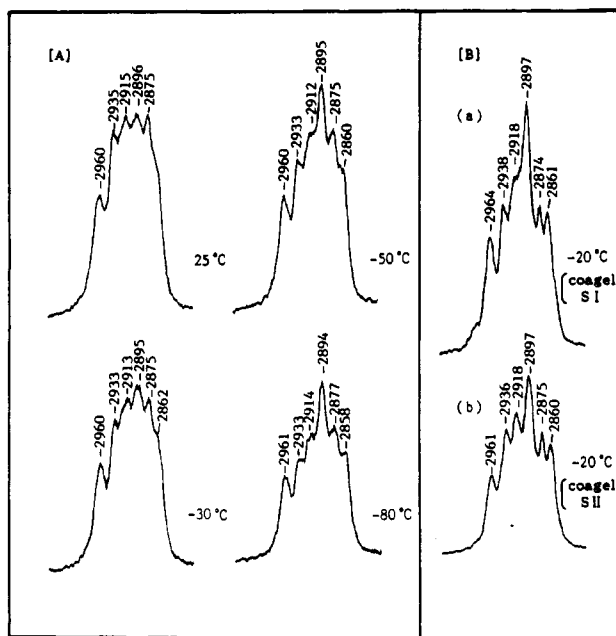


**Figure 7.** [A] Temperature dependence of the Raman bands for S III. [B] Raman spectra of coagels S I (a) and S II (b) at  $-20\text{ }^\circ\text{C}$  in the C-H stretching region.

Figure 7 shows the Raman spectra for S III at lower temperatures and for the coagels S I and S II in the C-H stretching region. For S III, the Raman band at  $2894\text{--}2896\text{ cm}^{-1}$  is found to increase in intensity as the sample is cooled below  $25\text{ }^\circ\text{C}$ . For the coagels S I and S II, the Raman bands at  $2897\text{ cm}^{-1}$  also differ from each other in intensity. This difference is ascribed to the difference in packing of the  $n$ -pentyl chains coming from stabilization of a specific rotational isomer.

**Hydration Effect on the Phosphodiester Conformation.** The present Raman scattering results demonstrate that the phosphodiester conformation of DPP in the coagel state depends upon the water content. The water/DPP mole ratios of S I and S II are 6 and 3.5, respectively. For S III, the OH stretching IR bands arising from water molecules were not observed, indicating that S III is essentially free of water. For phospholipid hydration, about

(35) Snyder, R. G. *J. Chem. Phys.* **1967**, *47*, 1316.

(36) Kawai, T.; Umemura, T.; Takenaka, T.; Kodama, M.; Seki, S. *J. Colloid Interface Sci.* **1985**, *103*, 56.

nine water molecules are tightly bound to the phosphate group.<sup>37</sup> The hydration number may be applied to the case of DPP. For the coagels S I and S II, the primary hydration site of DPP may be partially occupied by water molecules.

The Raman spectra of S III show that the GG and GT (or TT) forms coexist in the solid state at 25 °C and the preferential stabilization of the GG form occurs with a decrease in temperature. This observation implies that the GG form is stable relative to the GT (or TT) form in S III and the intramolecular free energy differences between the two conformations are small. The Raman spectra also reveal that the TT form is stabilized for the coagel S I and the GT form for the coagel S II, indicating that the extent of hydration of the phosphate moiety affects the conformational preference of DPP.

Recently, the thermodynamic quantities for the GG, GT, and TT forms of DMP have been calculated by Jayaram et al.<sup>33</sup> The calculation of DMP in free space has suggested that the intramolecular free energies favor the GG form relative to the GT and TT forms and that the free energy differences are within  $3k_B T$ . These results may be applied to DPP.

The IR and Raman studies for DMP<sup>12</sup> have suggested that the conformation in water is predominantly in the GG form. Conversely, depolarized Rayleigh scattering and vibrational spectra of DMP<sup>32</sup> have suggested that the GT and TT forms of the anion are highly populated.

The hydration shell model<sup>38-40</sup> has also been used by Jayaram et al.<sup>33</sup> to assume the relative conformational free energies of hydration of DMP. Analysis of the results suggests that the phosphodiester torsional angles are in the GG form rather than the GT and TT forms in the hydrated DMP and the conformational differences for the hydration free energies are small.

The stability of the GG form in the hydrated DMP does not explain the fact that the TT and GT forms are predominantly stabilized in the coagels S I and S II. However, we emphasize that the small conformational differences for the hydration free energies of DMP may be applied to DPP and enable the preference of the TT and GT forms in DPP owing to the hydration environment in the coagel state.

At the bilayer interface all hydrated water molecules are highly oriented and strongly restricted at the phosphate moiety for the DBP-H<sub>2</sub>O system.<sup>29</sup> A bilayer structure has also been confirmed for the lyotropic state of the DPP-H<sub>2</sub>O system by use of the X-ray diffraction method.<sup>30</sup> Thus, the DPP anion is also expected to form the highly ordered bilayer-type structure in the coagel state.

Therefore, we may assume that the hydration shell in the coagels S I and S II is much more rigid compared with that in bulk water and its structure depends upon the extent of hydration. In such a rigid hydration shell, the available conformational space of DPP is probably extremely restricted. The restricted conformational space may be associated with the number of water molecules in the rigid shell, which plays a significant role in the size of shell.<sup>41-43</sup> This restriction may cause the conformational preferences of the DPP phosphodiester torsional angles in the coagels, owing to the small conformational differences for the hydration free energies.

Detailed structural studies of the DPP-H<sub>2</sub>O complexes are desirable for clarification of the mechanism of preferential stabilization of the TT and GT forms in the DPP coagels.

## Conclusion

In the isotropic and lyotropic phases, very broad Raman bands at 270–272 cm<sup>-1</sup> appear and are ascribed to the accordion vibrational modes which are a consequence of the two extended pentyl chains.

The phase transition from the lyotropic state to the coagel phase leads to a marked variation in the accordion-like vibrational modes and is strongly dependent upon the water content in the samples. For S I in the coagel state, the accordion-like vibration is observed at 283–285 cm<sup>-1</sup>, while for the coagel S II it is split into two bands at 253–256 and 279–282 cm<sup>-1</sup>. Additionally, for S III the accordion-like vibration is observed at 253–260 cm<sup>-1</sup>. Assignment of the accordion-like vibration was made by normal coordinate analysis for three rotational isomers (GG, GT, and TT) about the P–O bonds. The accordion-like vibration at 283–285 cm<sup>-1</sup> for the coagel S I arises from the *all-trans-n*-pentyl chains of the TT form. For the coagel S II, the two split bands at 253–260 and 279–282 cm<sup>-1</sup> are due to the GT form. The former band arises from the extended *n*-pentyl chain in the gauche conformation about the P–O bonds, while the latter band arises from another extended chain in the trans conformation. For S III, the band at 253–256 cm<sup>-1</sup> is ascribed to the two *all-trans-n*-pentyl chains of the GG form. Preferential stabilization of a specific rotational isomer about the P–O bonds occurs and depends upon the water content. Therefore, the broad accordion-like vibration observed in the isotropic and lyotropic phases may consist of the accordion-like vibrations arising from the *all-trans-n*-pentyl chains for the GG, GT, and TT conformers. Stabilization of such a specific conformer is reflected in the observation of bands in the region of higher frequency in the Raman spectra.

*Acknowledgment.* We sincerely thank Dr. C. J. O'Connor of the University of Auckland, New Zealand, for helpful discussions.

(37) Tsai, Y.-S.; Ma, S.-M.; Kamaya, H.; Ueda, I. *Mol. Pharmacol.* **1987**, *31*, 623.

(38) Gibson, K. D.; Scheraga, H. A. *Proc. Natl. Acad. Sci. U.S.A.* **1967**, *58*, 420.

(39) Dunfield, L. G.; Burgess, A. W.; Scheraga, H. A. *J. Phys. Chem.* **1978**, *82*, 2601.

(40) Hodes, Z. I.; Nemethy, G.; Scheraga, H. A. *Biopolymers* **1979**, *18*, 1565.

(41) Lee, B.; Richards, F. M. *J. Mol. Biol.* **1971**, *55*, 379.

(42) Ponnuswamy, P. K.; Manavalan, P. *J. Theor. Biol.* **1976**, *60*, 481.

(43) Monavalan, P.; Ponnuswamy, P. K.; Srinivasan, A. R. *Biochem. J.* **1977**, *167*, 171.

(44) Shimanouchi, T. *Pure Appl. Chem.* **1963**, *7*, 131.